Optics Letters

Low-loss Kagome hollow-core fibers operating from the near- to the mid-IR

N. V. Wheeler,* T. D. Bradley, J. R. Hayes, M. A. Gouveia, S. Liang, Y. Chen, S. R. Sandoghchi, S. M. Abokhamis Mousavi, F. Poletti, M. N. Petrovich, and D. J. Richardson

Optoelectronics Research Centre, University of Southampton, Southampton SO17 1BJ, UK
**Corresponding author: n.v.wheeler@soton.ac.uk*

Received 31 January 2017; revised 28 April 2017; accepted 28 April 2017; posted 4 May 2017 (Doc. ID 285820); published 28 June 2017

We report the fabrication and characterization of Kagome hollow-core antiresonant fibers, which combine low attenuation (as measured at ~30 cm bend diameter) with a wide operating bandwidth and high modal purity. Record low attenuation values are reported: 12.3 dB/km, 13.9 dB/km, and 9.6 dB/km in three different fibers optimized for operation at 1 μm, 1.55 μm, and 2.5 μm, respectively. These fibers are excellent candidates for ultra-high power delivery at key laser wavelengths including 1.064 μm and 2.94 μm, as well as for applications in gas-based sensing and nonlinear optics.

Published by The Optical Society under the terms of the Creative Commons Attribution 4.0 License. Further distribution of this work must maintain attribution to the author(s) and the published article's title, journal citation, and DOI.

OCIS codes: (060.2280) Fiber design and fabrication; (060.5295) Photonic crystal fibers; (060.2390) Fiber optics, infrared; (060.4005) Microstructured fibers.

https://doi.org/10.1364/OL.42.002571

Hollow-core antiresonant fibers (HC-ARFs) form a subset of the expanding family of hollow-core photonic crystal fibers (HC-PCFs). A HC-ARF confines light in an air core in specific wavelength regions through antiresonance with the glass membranes which define the core boundary. The spectral regions where a HC-ARF can transmit light with low loss are therefore defined by the thickness of these membranes. As well as providing low-loss and octave-spanning spectral guidance in multiple spectral windows, HC-ARFs have been attracting increasing interest due to their large core diameters (typically several tens of micrometers and up to ~120 μm), ultra-low nonlinearity, and low group velocity dispersion. Due to these properties, HC-ARFs are excellent candidates for high-power beam delivery, in particular of ultrashort pulses and gas-based nonlinear optics applications [1–3].

Antiresonant guidance opens up a high degree of flexibility in fiber design, and several HC-ARF structures have been reported to date [4–6]. Kagome hollow-core antiresonant fibers (K-ARFs) are the most highly developed HC-ARF structure and were initially described in 2002 [7]; further improvements in fabrication and optical performance, as well as increased insight into this type of guidance mechanism, were provided in 2007 [8]. Until recently, K-ARFs have typically been associated with attenuation at the level of ~dB/m; however, substantial efforts to reduce the overlap of the core guided modes with the core surround through engineering the shape of the core boundary have resulted in dramatic loss reduction [9]. In particular, focused efforts to achieve a core boundary shape with a highly negative curvature have led to remarkable low attenuation values of 17 dB/km [10] and very recently, 8.5 dB/km [11], both around the 1 μm wavelength region. As such, the attenuation of K-ARFs at wavelengths around 1 μm or below can now compete with, or even be lower than, losses achieved in hollow-core photonic bandgap fibers [12]. Yet, in these record-low-loss fibers, it has so far proven extremely challenging to combine low loss with low bend sensitivity and wide operating bandwidth. For example, the 17 dB/km K-ARF [10] has a low loss bandwidth of only ~10 nm and therefore compromises on one of the key parameters that is typically exploited in a K-ARF, and the 8.5 dB/km K-ARF in Ref. [11] has high bend loss, so that the low attenuation value is measured with a 70 cm bend diameter. As such, further progress is required to simultaneously achieve very low loss over a wide spectral range along with low bend sensitivity, while producing long, uniform lengths of fiber.

In this Letter, we report the fabrication of three K-ARFs, designed for operation at 1 μm [13], 1.55 μm, and 2.5 μm, respectively, that all have record low attenuation (as measured at ~30 cm bend diameter) while maintaining broad operating bandwidths, and therefore represent a new state of the art for K-ARFs. This is achieved, in part, by operating in the fundamental transmission window, which enables a wide, low-loss operating bandwidth and has the added benefit of reducing the sensitivity of the fiber to bend loss; measurements on our 1.55 μm K-ARF show this fiber demonstrates record low bend loss for a K-ARF. We also report detailed measurements of the modal properties of our 1.55 μm K-ARF, which indicate that these new K-ARFs can have a high modal purity if appropriate launch conditions are used. The combination of ultra-low loss, low bend sensitivity, large mode field diameter, and high modal purity render these fibers excellent for high-power laser delivery at key wavelengths including 1.064 μm and 2.94 μm, where, to the best of our knowledge, our

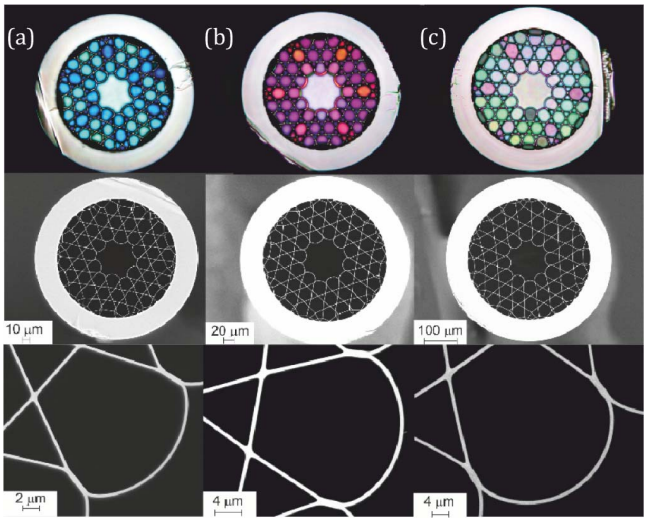

Fig. 1. (a), (b), and (c) Optical microscope images (top row) and SEM images of the full fiber (middle row) and the core surround (bottom row) of fibers A, B, and C, respectively.

K-ARF demonstrates the lowest optical loss achieved in any hollow-core fiber reported to date.

The K-ARFs reported here all have a seven-cell core design and were fabricated using the conventional stack and draw technique. The capillary dimensions in the stack were designed so that in the final fiber, the target wavelength would be in the fundamental transmission window in order to maximize the low-loss operating bandwidth and to reduce bend loss. Operation in this spectral window requires the silica membranes which surround the air core to be substantially thinner than if the fiber is designed for operation in a higher-order spectral window, and this makes fabrication of a core membrane more challenging, particularly if targeting a high degree of negative curvature. Therefore, in the fiber draw process it is essential to carefully control the difference between the core and cladding pressures, as well as the draw tension, to obtain a core surround with a negative curvature shape.

Scanning electron microscope (SEM) images of the three fibers (referred to as A, B, and C for low loss at 1 μm, 1.55 μm, and 2.5 μm, respectively) are shown in Figs. 1(a)–1(c). A summary of the key properties, both structural and optical, is presented in Table 1. These fibers were each drawn from separate canes (with very similar structures) and the core size scales with the wavelength of the fundamental guidance window. The attenuation spectra (calculated using cutback measurements) for the three fibers are shown in Fig. 2. For clarity, the attenuation of only the fundamental spectral window is presented, but in each case the loss in the higher-order windows was found to be higher than in the fundamental spectral window; for example, in fiber B, the minimum loss in the first higher-order window is 62 dB/km at 878 nm. Fibers A and B were measured using a white light source (WLS) and optical spectrum analyzer (OSA). The WLS was coupled into these K-ARFs using a large mode area fiber with a similar mode field diameter to the fundamental mode of the K-ARF. The mode field diameters of our fibers were estimated to be ~73% of the core diameter [14]. Fiber C was measured using an in-house built mid-infrared supercontinuum source [15]. The fiber output of this source was butt-coupled directly to fiber C in order to carry out the loss measurements, and due to a large mode field diameter mismatch (~6.5 μm for the supercontinuum output compared to ~75 μm for fiber C), this measurement does suffer from higher modal noise, which is evident in the loss spectrum. A Yokogawa AQ6376 OSA was used for detection at mid-infrared (IR) wavelengths. For all the loss measurements, the fibers were loosely coiled in ~30 cm diameter loops. From these measurements, the minimum losses of fibers A, B, and C were found to be 12.3 dB/km, 13.9 dB/km, and 9.6 dB/km, and each fiber has a low loss (3 dB) bandwidth of at least 150 nm. These fibers all represent record low loss values for K-ARFs (at 1 μm, considering the bend diameter in the measurement) in their respective spectral regions, and fibers B and C represent new record low loss values for any HC-ARF in their

Table 1. Key Structural and Optical Properties of Fibers A, B, and C

	Core Diameter (μm)	Core Wall Thickness (nm)	Minimum Loss Wavelength (nm)	Minimum Loss (dB/km)	3 dB Bandwidth (nm)	Curvature Parameter "b"
Fiber A	43	375	1010	12.3 ± 2.2	150	0.5
Fiber B	64	600	1566	13.9 ± 1.0	198	0.57
Fiber C	97	975	2462	9.6 ± 3.0	191	0.69

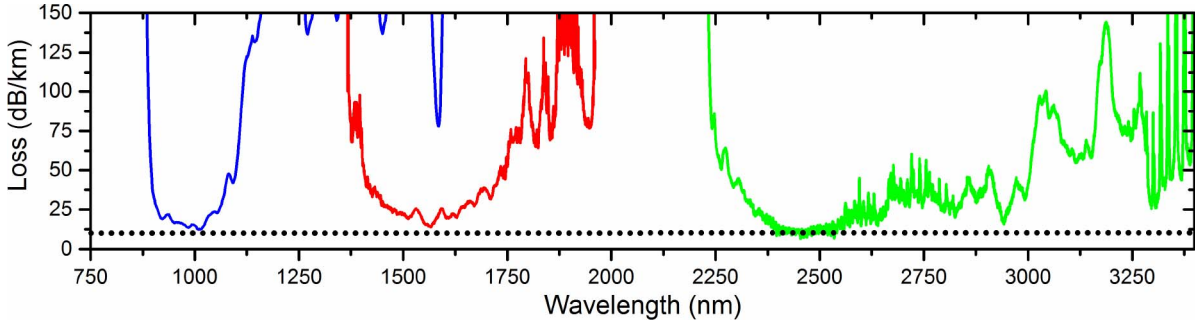

Fig. 2. Attenuation spectra of fibers A, B, and C (blue, red, and green lines, respectively) measured using the cutback technique. Dotted black line indicates loss equal to 10 dB/km.

minimum loss windows. The measurement uncertainties in Table 1 were estimated by considering the variation in transmission spectra recorded using three different fiber cleaves performed at each length for each fiber, and also the cutback fiber lengths used (63–5 m, 148–15 m, and 100–10 m for fibers A–C, respectively). It is also noteworthy that the minimum loss of fiber C at 2.94 μm, which coincides with the Er:YAG high-power laser source, is 18.6 dB/km, which we believe represents a new record low loss for any hollow-core fiber at this wavelength. Furthermore, fiber C has an attenuation below 150 dB/km across a wide spectral region spanning from 2.25 to beyond 3.4 μm. The measurement of fiber C is truncated at the long wavelength edge due to the range limitation of the OSA used for detection; however, measurements of shorter lengths using an Fourier transform infrared spectrometer show transmission up to 4.7 μm. The attenuation curve for each fiber is clearly structured as is common with K-ARFs, as the resonances of the core guided modes with silica cladding nodes increase the fiber loss at specific wavelengths. The attenuation of fiber C also has loss peaks due to water vapor and carbon dioxide (~2.5–2.85 μm) and hydrogen chloride gas absorption (~3.3–3.4 μm); these species are known to be present in as-fabricated hollow-core photonic crystal fibers, and can be reduced or eliminated by purging the fiber with dry gas [16,17].

Table 1 also shows the calculated core curvature parameter "b" (as defined in Ref. [10]) for each fiber. This parameter increases as the core membrane thickness increases from fibers A to C, as the fundamental transmission window is shifted to longer wavelengths. In the previous state-of-the-art K-ARFs, b is equal to 1 and 0.9 (in Refs. [10] and [11], respectively), and in these papers the authors argue that increasing b leads to reduced loss. For fibers A, B, and C, we can see that although b is significantly lower than 1, the loss is still reduced. We believe that this is because the core curvature parameter cannot be considered alone when predicting the minimum loss structure; in fact, the shape and size of the nodes in the core surround, in combination with the core curvature, will define the minimum loss. Additionally, longitudinal uniformity along the fiber lengths is important to avoid defect-induced losses [18], and for our fibers, longitudinal uniformity was confirmed for fibers A and B using an optical time domain reflectometry.

Fiber B was chosen for a more detailed study as its low loss operation at 1550 nm makes it amenable for measurement with our S^2 setup [19], which enables analysis of the modal content of the fiber in near real time. The S^2 results for a 133 m length of fiber, cut back to 5 m, are shown in Fig. 3. These measurements were taken using a free-space, lens-optimized launch into the input of the fiber to ensure maximum coupling into the fundamental mode, and as the measurements were taken as a cutback, the input coupling conditions for both measurements are the same. The S^2 measurement bandwidth (1555–1575 nm) was centered on the lowest transmission loss region for this fiber, and the laser source was swept in 1 pm steps at a rate of 500 pm/s. From Fig. 3 it is clear that, as expected [20], fiber B supports several modes. However, with appropriate coupling into the fiber, only a few higher-order mode groups (HOMs) are present after a 5 m length, and in total the HOM content is suppressed to approximately 18 dB below the fundamental mode (corresponding to ~1.6% of the total power being transmitted in HOMs). Note that in both plots in Fig. 3, unlabeled peaks correspond to double reflections from different

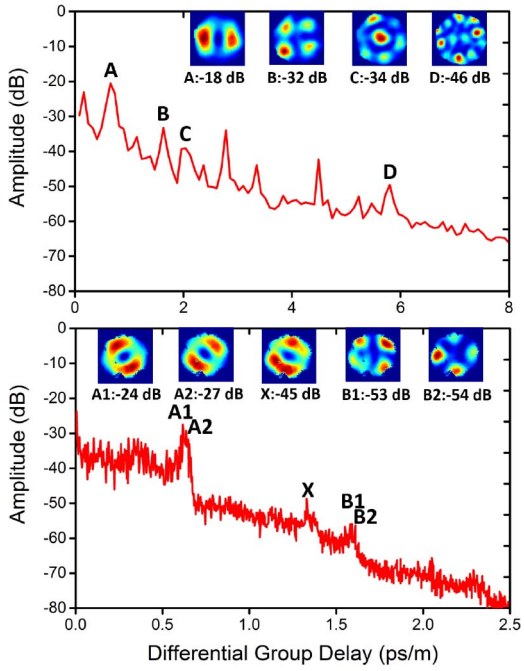

Fig. 3. S^2 measurements on 5 m (top) and 133 m (bottom) lengths of fiber B. Amplitude peaks corresponding to different modes propagating in the fiber are labeled; mode groups A and B correspond to the LP_{11} and LP_{21} modes, respectively. Unlabeled peaks correspond to double reflections in the measurement setup [18]. Modal images for each fiber length are shown inset to each plot along with total power amplitude (MPI) in each mode compared to the fundamental mode power.

components in the measurement setup, which are discussed in detail elsewhere [21]. Over a longer length of 133 m, the higher-order mode extinction is ~24 dB, While this is an increase, this clearly shows that the differential loss between the LP_{11} mode group and the fundamental mode is not especially high; from this measurement the LP_{11} mode loss is estimated to be ~50 dB/km. This ratio of LP_{11} mode loss to fundamental mode loss (~3.6) is comparable with the results of our previous study of modal content in K-ARFs [20]. One feature to note is that over the 133m length, a mode (labeled "X") is present with a differential group delay between that of the LP_{11} and LP_{21} mode groups; we believe this arises due to a discrete event where a very small amount of power is coupled between the LP_{11} and LP_{21} modes. As the core size of our fibers scales with wavelength, we believe that similar modal properties would be recorded for fibers A and C.

Figure 4 shows the bend loss measurements for fiber B at four different wavelengths [three in the fundamental transmission window and one (850 nm) in the first higher-order transmission window of the fiber]. These measurements were carried out using a WLS and by comparing the transmission of a very loosely coiled 5 m length of fiber B with the transmission as tighter bends were introduced along the fiber length, without changing the input or output coupling conditions. In the lowest loss spectral region around 1550 nm, the bend loss is very low for this fiber type, becoming significant compared with the measured cutback loss reported above at bend diameters ~16 cm. From comparison with state-of-the-art fibers in the literature [22] with a similar core size, and which provide low loss at similar wavelengths, we believe this sets a record low bend sensitivity for

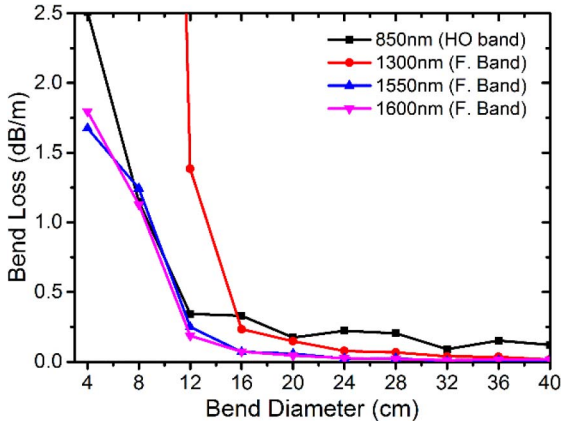

Fig. 4. Bend loss measurements of fiber B at four different wavelengths, indicating low bend sensitivity at 1550 nm and 1600 nm.

a K-ARF. Note, we have also measured the bend sensitivity of fiber A (see Ref. [13]), and this fiber also shows reduced bend loss compared to the previous state-of-the-art K-ARF operating around 1 μm [11]; however, the bend loss becomes significant as compared to the cutback loss at a bend diameter ~24 cm. Considering that the structures of fibers A and B are very similar, the origin of this difference will be investigated further. From Fig. 4, it is clear that, as expected, the bend sensitivity increases at wavelengths closer to the edge of the transmission window, where the wavelength is closer to resonance, and also that the bend sensitivity increases in the higher-order transmission window (as the wavelength is reduced relative to the core diameter). Even with this record low bend sensitivity, improvement in this optical property would be beneficial to many applications, such as the fabrication of compact fiber-based gas sensors.

The fibers presented here demonstrate low loss (measured at ~30 cm bend diameter), wide operating bandwidth, and large mode field diameter. Furthermore, detailed measurements of our fiber optimized for operation around 1.55 μm demonstrate record low bend loss for a K-ARF and high modal purity (with appropriate launch conditions). Therefore, we believe these fibers represent a new state of the art for K-ARFs. In the 1 μm spectral region, our fiber presents comparable loss to state-of-the-art hollow-core photonic bandgap fibers [12], and at 1.55 μm, our fiber has the lowest loss for any HC-ARF. At 2.94 μm, our fiber represents the lowest-loss hollow-core fiber of any design. These fibers are highly suited for ultra-high power beam delivery from the near- to the mid-IR. Recently, several new low-loss HC-ARFs have been reported [23–25], and in particular "nodeless" designs hold high promise for further loss reduction, as they have highly simplified structures and remove the attenuating resonances that are present in the cladding of a K-ARF. However, the optimal structure which will provide the best complete set of optical properties is still an open question, and further work on both HC-ARF structures is ongoing.

Funding. Royal Society; Engineering and Physical Sciences Research Council (EPSRC) National Photonics Hub (EP/N00762X/1).

Acknowledgment. N.V. Wheeler and F. Poletti acknowledge support from Royal Society University Research Fellowships.

The data for this paper can be found at http://doi.org/10.5258/SOTON/405210.

REFERENCES

1. C. Saraceno, F. Emaury, A. Diebold, I. Graumann, M. Golling, and U. Keller, Proc. SPIE **9835**, 98350X (2016).
2. B. Debord, M. Alharbi, L. Vincetti, A. Husakou, C. Fourcade-Dutin, C. Hoenninger, E. Mottay, F. Gerome, and F. Benabid, Opt. Express **22**, 10735 (2014).
3. C. Wang, N. V. Wheeler, C. Fourcade-Dutin, M. Grogan, T. D. Bradley, B. R. Washburn, F. Benabid, and K. L. Corwin, Appl. Opt. **52**, 5430 (2013).
4. F. Couny, F. Benabid, and P. S. Light, Opt. Lett. **31**, 3574 (2006).
5. F. Yu, W. J. Wadsworth, and J. C. Knight, Opt. Express **20**, 11153 (2012).
6. A. N. Kolyadin, A. F. Kosolapov, A. D. Pryamikov, A. S. Biriukov, V. G. Plotnichenko, and E. M. Dianov, Opt. Express **21**, 9514 (2013).
7. F. Benabid, J. C. Knight, G. Antonopoulos, and P. St.J. Russell, Science **298**, 399 (2002).
8. F. Couny, F. Benabid, P. J. Roberts, P. S. Light, and M. G. Raymer, Science **318**, 1118 (2007).
9. Y. Y. Wang, N. V. Wheeler, F. Couny, P. J. Roberts, and F. Benabid, Opt. Lett. **36**, 669 (2011).
10. B. Debord, M. Alharbi, T. Bradley, C. Fourcade-Dutin, Y. Y. Wang, L. Vincetti, F. Gerome, and F. Benabid, Opt. Express **21**, 28597 (2013).
11. B. Debord, M. Maurel, A. Amsanpally, M. Adnan, B. Beaudou, J. M. Blondy, L. Vincetti, F. Gerome, and F. Benabid, Proc. SPIE **10094**, 100941M (2017).
12. Y. Chen, H. C. H. Mulvad, S. R. Sandoghchi, E. Numkam, T. D. Bradley, J. R. Hayes, N. V. Wheeler, G. T. Jasion, S. U. Alam, F. Poletti, M. N. Petrovich, and D. J. Richardson, *Conference on Lasers and Electro-Optics* (Optical Society of America, 2016), paper STu4P.1.
13. N. V. Wheeler, T. D. Bradley, J. R. Hayes, M. A. Gouveia, Y. Chen, S. R. Sandohgchi, F. Poletti, M. N. Petrovich, and D. J. Richardson, *Advanced Photonics Congress* (Optical Society of America, 2016), paper SoM3F.2.
14. E. A. J. Marcatili and R. A. Schmeltzer, Bell Syst. Tech. J. **43**, 1783 (1964).
15. A. M. Heidt, J. H. V. Price, C. Baskiotis, J. S. Feehan, Z. Li, S. U. Alam, and D. J. Richardson, Opt. Express **21**, 24281 (2013).
16. N. V. Wheeler, A. M. Heidt, N. K. Baddela, E. N. Fokoua, J. R. Hayes, S. R. Sandoghchi, F. Poletti, M. N. Petrovich, and D. J. Richardson, Opt. Lett. **39**, 295 (2014).
17. N. V. Wheeler, M. N. Petrovich, N. K. Baddela, J. R. Hayes, E. N. Fokoua, F. Poletti, and D. J. Richardson, *Conference on Lasers and Electro-Optics* (Optical Society of America, 2012), paper CM3N.5.
18. S. R. Sandoghchi, M. N. Petrovich, D. R. Gray, Y. Chen, N. V. Wheeler, T. D. Bradley, N. H. L. Wong, G. Jasion, J. R. Hayes, E. Numkam Fokoua, M. Botelho Alonso Gouveia, S. M. Abokhamis Mousavi, D. J. Richardson, and F. Poletti, Opt. Express **23**, 27960 (2015).
19. D. R. Gray, M. N. Petrovich, S. R. Sandoghchi, N. V. Wheeler, N. K. Baddela, G. T. Jasion, T. Bradley, D. J. Richardson, and F. Poletti, IEEE Photon. Technol. Lett. **28**, 1034 (2016).
20. T. D. Bradley, N. V. Wheeler, G. T. Jasion, D. R. Gray, J. R. Hayes, M. Botelho Alonso, S. M. Sandoghchi, Y. Chen, F. Poletti, D. J. Richardson, and M. N. Petrovich, Opt. Express **24**, 15798 (2016).
21. D. R. Gray, S. R. Sandoghchi, N. V. Wheeler, N. K. Baddela, G. T. Jasion, M. N. Petrovich, F. Poletti, and D. J. Richardson, *Optical Fiber Communication Conference* (Optical Society of America, 2015), paper W4I.6.
22. M. Alharbi, T. Bradley, B. Debord, C. Fourcade-Dutin, D. Ghosh, L. Vincetti, F. Gerome, and F. Benabid, Opt. Express **21**, 28609 (2013).
23. J. R. Hayes, F. Poletti, S. Abokhamis Mousavi, N. V. Wheeler, N. K. Baddela, and D. J. Richardson, J. Lightwave Technol. **35**, 437 (2017).
24. B. Debord, A. Amsanpally, M. Chafer, A. Bas, M. Maurel, J.-M. Blondy, E. Huggonot, L. Vincetti, F. Gerome, and F. Benabid, Optica **4**, 209 (2017).
25. M. Michieletto, J. K. Lyngso, C. Jakobsen, J. Laesgaard, O. Bang, and T. T. Alkeskjold, Opt. Express **24**, 7103 (2016).

152.78.9.68 {ts '2020-05-07 11:50:35'}